

Fermi National Accelerator Laboratory

FERMILAB Pub-94/126-E

**W Boson + Jet Angular Distribution
in $p\bar{p}$ Collisions at $\sqrt{s} = 1.8$ TeV**

F. Abe et al
The CDF Collaboration

*Fermi National Accelerator Laboratory
P.O. Box 500, Batavia, Illinois 60510*

May 1994

Submitted to *Physical Review Letters*

Disclaimer

This report was prepared as an account of work sponsored by an agency of the United States Government. Neither the United States Government nor any agency thereof, nor any of their employees, makes any warranty, express or implied, or assumes any legal liability or responsibility for the accuracy, completeness, or usefulness of any information, apparatus, product, or process disclosed, or represents that its use would not infringe privately owned rights. Reference herein to any specific commercial product, process, or service by trade name, trademark, manufacturer, or otherwise, does not necessarily constitute or imply its endorsement, recommendation, or favoring by the United States Government or any agency thereof. The views and opinions of authors expressed herein do not necessarily state or reflect those of the United States Government or any agency thereof.

W Boson + Jet Angular Distribution in $p\bar{p}$ Collisions at $\sqrt{s} = 1.8$ TeV

F. Abe,¹³ M. G. Albrow,⁷ D. Amidei,¹⁶ J. Antos,²⁸ C. Anway-Wiese,⁴ G. Apollinari,²⁶ H. Areti,⁷ P. Auchincloss,²⁵ F. Azfar,²¹ P. Azzi,²⁰ N. Bacchetta,¹⁸ W. Badgett,¹⁶ M. W. Bailey,¹⁸ J. Bao,³⁴ P. de Barbaro,²⁵ A. Barbaro-Galtieri,¹⁴ V. E. Barnes,²⁴ B. A. Barnett,¹² P. Bartalini,²³ G. Bauer,¹⁵ T. Baumann,⁹ F. Bedeschi,²³ S. Behrends,³ S. Belforte,²³ G. Bellettini,²³ J. Bellinger,³³ D. Benjamin,³² J. Benloch,¹⁵ J. Bensinger,³ D. Benton,²¹ A. Beretvas,⁷ J. P. Berge,⁷ S. Bertolucci,⁸ A. Bhatti,²⁶ K. Biery,¹¹ M. Binkley,⁷ F. Bird,²⁹ D. Bisello,²⁰ R. E. Blair,¹ C. Blocker,²⁹ A. Bodek,²⁵ V. Bolognesi,²³ D. Bortoletto,²⁴ C. Boswell,¹² T. Boulos,¹⁴ G. Brandenburg,⁹ E. Buckley-Geer,⁷ H. S. Budd,²⁵ K. Burkett,¹⁶ G. Busetto,²⁰ A. Byon-Wagner,⁷ K. L. Byrum,¹ C. Campagnari,⁷ M. Campbell,¹⁶ A. Caner,⁷ W. Carithers,¹⁴ D. Carlsmith,³³ A. Castro,²⁰ Y. Cen,²¹ F. Cervelli,²³ J. Chapman,¹⁶ M.-T. Cheng,²⁸ G. Chiarelli,⁸ T. Chikamatsu,³¹ S. Cihangir,⁷ A. G. Clark,²³ M. Cobal,²³ M. Contreras,⁵ J. Conway,²⁷ J. Cooper,⁷ M. Cordelli,⁸ D. Crane,⁷ J. D. Cunningham,³ T. Daniels,¹⁵ F. DeJongh,⁷ S. Delchamps,⁷ S. Dell'Agnello,²³ M. Dell'Orso,²³ L. Demortier,²⁶ B. Denby,²³ M. Deninno,² P. F. Derwent,¹⁶ T. Devlin,²⁷ M. Dickson,²⁵ S. Donati,²³ R. B. Drucker,¹⁴ A. Dunn,¹⁶ K. Einsweiler,¹⁴ J. E. Elias,⁷ R. Ely,¹⁴ E. Engels, Jr.,²² S. Eno,⁵ D. Errede,¹⁰ S. Errede,¹⁰ Q. Fan,²⁵ B. Farhat,¹⁵ I. Fiori,² B. Flaugher,⁷ G. W. Foster,⁷ M. Franklin,⁹ M. Frautschi,¹⁸ J. Freeman,⁷ J. Friedman,¹⁵ H. Frisch,⁵ A. Fry,²⁹ T. A. Fuess,¹ Y. Fukui,¹³ S. Funaki,³¹ G. Gagliardi,²³ S. Galeotti,²³ M. Gallinaro,²⁰ A. F. Garfinkel,²⁴ S. Geer,⁷ D. W. Gerdes,¹⁶ P. Giannetti,²³ N. Giokaris,²⁶ P. Giromini,⁸ L. Gladney,²¹ D. Glenzinski,¹² M. Gold,¹⁸ J. Gonzalez,²¹ A. Gordon,⁹ A. T. Goshaw,⁶ K. Goulianatos,²⁶ H. Grassmann,⁶ A. Grewal,²¹ G. Grieco,²³ L. Groer,²⁷ C. Gross-Pilcher,⁵ C. Haber,¹⁴ S. R. Hahn,⁷ R. Hamilton,⁹ R. Handler,³³ R. M. Hans,³⁴ K. Hara,³¹ B. Harral,²¹ R. M. Harris,⁷ S. A. Hauger,⁶ J. Hauser,⁴ C. Hawk,²⁷ J. Heinrich,²¹ D. Cronin-Hennessy,⁶ R. Hollebeek,²¹ L. Holloway,¹⁰ A. Hölscher,¹¹ S. Hong,¹⁶ G. Houk,²¹ P. Hu,²² B. T. Huffman,²² R. Hughes,²⁵ P. Hurst,⁹ J. Huston,¹⁷ J. Huth,⁹ J. Hylen,⁷ M. Incagli,²³ J. Incandela,⁷ H. Iso,³¹ H. Jensen,⁷ C. P. Jessop,⁹ U. Joshi,⁷ R. W. Kadel,¹⁴ E. Kajfasz,^{7a} T. Kamon,³⁰ T. Kaneko,³¹ D. A. Kardelis,¹⁰ H. Kasha,³⁴ Y. Kato,¹⁹ L. Keeble,³⁰ R. D. Kennedy,²⁷ R. Kephart,⁷ P. Kesten,¹⁴ D. Kestenbaum,⁹ R. M. Keup,¹⁰ H. Keutelian,⁷ F. Keyvan,⁴ D. H. Kim,⁷ H. S. Kim,¹¹ S. B. Kim,¹⁶ S. H. Kim,³¹ Y. K. Kim,¹⁴ L. Kirsch,³ P. Koehn,²⁵ K. Kondo,³¹ J. Konigsberg,⁹ S. Kopp,⁵ K. Kordas,¹¹ W. Koska,⁷ E. Kovacs,^{7a} W. Kowald,⁶ M. Krasberg,¹⁶ J. Kroll,⁷ M. Kruse,²⁴ S. E. Kuhlmann,¹ E. Kuns,²⁷ A. T. Laasanen,²⁴ S. Lammel,⁴ J. I. Lamoureux,³ T. LeCompte,¹⁰ S. Leone,²³ J. D. Lewis,⁷ P. Limon,⁷ M. Lindgren,⁴ T. M. Liss,¹⁰ N. Lockyer,²¹ O. Long,²¹ M. Loretto,²⁰ E. H. Low,²¹ J. Lu,³⁰ D. Lucchesi,²³ C. B. Luchini,¹⁰ P. Lukens,⁷ P. Maas,³³ K. Maeshima,⁷ A. Maghakian,²⁶ P. Maksimovic,¹⁵ M. Mangano,²³ J. Mansour,¹⁷ M. Mariotti,²³ J. P. Marriner,⁷ A. Martin,¹⁰ J. A. J. Matthews,¹⁸ R. Mattingly,¹⁵ P. McIntyre,³⁰

Submitted to Phys. Rev. Lett. May 17, 1994.

P. Melese,²⁶ A. Menzione,²³ E. Meschi,²³ G. Michail,⁹ S. Mikamo,¹³ M. Miller,⁵
 R. Miller,¹⁷ T. Mimashi,³¹ S. Miscetti,⁸ M. Mishina,¹³ H. Mitsushio,³¹ S. Miyashita,³¹
 Y. Morita,¹³ S. Moulding,²⁶ J. Mueller,²⁷ A. Mukherjee,⁷ T. Muller,⁴ P. Musgrave,¹¹
 L. F. Nakae,²⁹ I. Nakano,³¹ C. Nelson,⁷ D. Neuberger,⁴ C. Newman-Holmes,⁷
 L. Nodulman,¹ S. Ogawa,³¹ S. H. Oh,⁶ K. E. Ohl,³⁴ R. Oishi,³¹ T. Okusawa,¹⁹
 C. Pagliarone,²³ R. Paoletti,²³ V. Papadimitriou,⁷ S. Park,⁷ J. Patrick,⁷ G. Paulett,²³
 M. Paulini,¹⁴ L. Pescara,²⁰ M. D. Peters,¹⁴ T. J. Phillips,⁶ G. Piacentino,² M. Pillai,²⁵
 R. Plunkett,⁷ L. Pondrom,³³ N. Produit,¹⁴ J. Proudfoot,¹ F. Ptohos,⁹ G. Punzi,²³
 K. Ragan,¹¹ F. Rimondi,² L. Ristori,²³ M. Roach-Bellino,³² W. J. Robertson,⁶
 T. Rodrigo,⁷ J. Romano,⁵ L. Rosenson,¹⁵ W. K. Sakumoto,²⁵ D. Saltzberg,⁵
 A. Sansoni,⁸ V. Scarpine,³⁰ A. Schindler,¹⁴ P. Schlabach,⁹ E. E. Schmidt,⁷
 M. P. Schmidt,³⁴ O. Schneider,¹⁴ G. F. Sciacca,²³ A. Scribano,²³ S. Segler,⁷
 S. Seidel,¹⁸ Y. Seiya,³¹ G. Sganos,¹¹ A. Sgolacchia,² M. Shapiro,¹⁴ N. M. Shaw,²⁴
 Q. Shen,²⁴ P. F. Shepard,²² M. Shimojima,³¹ M. Shochet,⁵ J. Siegrist,²⁹ A. Sill,^{7a}
 P. Sinervo,¹¹ P. Singh,²² J. Skarha,¹² K. Sliwa,³² D. A. Smith,²³ F. D. Snider,¹²
 L. Song,⁷ T. Song,¹⁶ J. Spalding,⁷ L. Spiegel,⁷ P. Sphicas,¹⁵ A. Spies,¹² L. Stanco,²⁰
 J. Steele,³³ A. Stefanini,²³ K. Strahl,¹¹ J. Strait,⁷ D. Stuart,⁷ G. Sullivan,⁵
 K. Sumorok,¹⁵ R. L. Swartz, Jr.,¹⁰ T. Takahashi,¹⁹ K. Takikawa,³¹ F. Tartarelli,²³
 W. Taylor,¹¹ Y. Teramoto,¹⁹ S. Tether,¹⁵ D. Theriot,⁷ J. Thomas,²⁹ T. L. Thomas,¹⁸
 R. Thun,¹⁶ M. Timko,³² P. Tipton,²⁵ A. Titov,²⁶ S. Tkaczyk,⁷ K. Tollefson,²⁵
 A. Tollestrup,⁷ J. Tonnison,²⁴ J. F. de Troconiz,⁹ J. Tseng,¹² M. Turcotte,²⁹
 N. Turini,² N. Uemura,³¹ F. Ukegawa,²¹ G. Unal,²¹ S. van den Brink,²² S. Vej-
 cik, III,¹⁶ R. Vidal,⁷ M. Vondracek,¹⁰ R. G. Wagner,¹ R. L. Wagner,⁷ N. Wainer,⁷
 R. C. Walker,²⁵ G. Wang,²³ J. Wang,⁵ M. J. Wang,²⁸ Q. F. Wang,²⁶ A. Warburton,¹¹
 G. Watts,²⁵ T. Watts,²⁷ R. Webb,³⁰ C. Wendt,³³ H. Wenzel,¹⁴ W. C. Wester, III,¹⁴
 T. Westhusing,¹⁰ A. B. Wicklund,¹ E. Wicklund,⁷ R. Wilkinson,²¹ H. H. Williams,²¹
 P. Wilson,⁵ B. L. Winer,²⁵ J. Wolinski,³⁰ D. Y. Wu,¹⁶ X. Wu,²³ J. Wyss,²⁰ A. Yagil,⁷
 W. Yao,¹⁴ K. Yasuoka,³¹ Y. Ye,¹¹ G. P. Yeh,⁷ P. Yeh,²⁸ M. Yin,⁶ J. Yoh,⁷ T. Yoshida,¹⁹
 D. Yovanovitch,⁷ I. Yu,³⁴ J. C. Yun,⁷ A. Zanetti,²³ F. Zetti,²³ L. Zhang,³³ S. Zhang,¹⁵
 W. Zhang,²¹ and S. Zucchelli²

(CDF Collaboration)

¹ Argonne National Laboratory, Argonne, Illinois 60439

² Istituto Nazionale di Fisica Nucleare, University of Bologna, I-40126 Bologna, Italy

³ Brandeis University, Waltham, Massachusetts 02254

⁴ University of California at Los Angeles, Los Angeles, California 90024

⁵ University of Chicago, Chicago, Illinois 60637

⁶ Duke University, Durham, North Carolina 27708

⁷ Fermi National Accelerator Laboratory, Batavia, Illinois 60510

⁸ Laboratori Nazionali di Frascati, Istituto Nazionale di Fisica Nucleare, I-00044 Frascati, Italy

⁹ Harvard University, Cambridge, Massachusetts 02138

¹⁰ University of Illinois, Urbana, Illinois 61801

¹¹ *Institute of Particle Physics, McGill University, Montreal H3A 2T8, and University of Toronto, Toronto M5S 1A7, Canada*

¹² *The Johns Hopkins University, Baltimore, Maryland 21218*

¹³ *National Laboratory for High Energy Physics (KEK), Tsukuba, Ibaraki 305, Japan*

¹⁴ *Lawrence Berkeley Laboratory, Berkeley, California 94720*

¹⁵ *Massachusetts Institute of Technology, Cambridge, Massachusetts 02139*

¹⁶ *University of Michigan, Ann Arbor, Michigan 48109*

¹⁷ *Michigan State University, East Lansing, Michigan 48824*

¹⁸ *University of New Mexico, Albuquerque, New Mexico 87131*

¹⁹ *Osaka City University, Osaka 588, Japan*

²⁰ *Universita di Padova, Istituto Nazionale di Fisica Nucleare, Sezione di Padova, I-35131 Padova, Italy*

²¹ *University of Pennsylvania, Philadelphia, Pennsylvania 19104*

²² *University of Pittsburgh, Pittsburgh, Pennsylvania 15260*

²³ *Istituto Nazionale di Fisica Nucleare, University and Scuola Normale Superiore of Pisa, I-56100 Pisa, Italy*

²⁴ *Purdue University, West Lafayette, Indiana 47907*

²⁵ *University of Rochester, Rochester, New York 14627*

²⁶ *Rockefeller University, New York, New York 10021*

²⁷ *Rutgers University, Piscataway, New Jersey 08854*

²⁸ *Academia Sinica, Taiwan 11529, Republic of China*

²⁹ *Superconducting Super Collider Laboratory, Dallas, Texas 75237*

³⁰ *Texas A&M University, College Station, Texas 77843*

³¹ *University of Tsukuba, Tsukuba, Ibaraki 305, Japan*

³² *Tufts University, Medford, Massachusetts 02155*

³³ *University of Wisconsin, Madison, Wisconsin 53706*

³⁴ *Yale University, New Haven, Connecticut 06511*

Abstract

The W +jet angular distribution is measured using $W \rightarrow e\nu$ events recorded with the Collider Detector at Fermilab (CDF) during the 1988-89 and 1992-93 Tevatron runs. The data agree well with both a leading order and a next-to-leading order theoretical prediction. The shape of the angular distribution is similar to that observed in photon+jet data, and significantly different from that observed in dijet data.

PACS numbers: 13.85.Qk, 14.70.Fm, 12.38.Qk

Events in which a W boson is produced in association with quarks or gluons (jets) provide a good test of perturbative quantum chromodynamics (QCD). At the Fermilab Tevatron, W +jet events are produced predominantly by quark exchange processes ($gq \rightarrow Wq'$ and $q\bar{q} \rightarrow Wg$). The spin- $\frac{1}{2}$ propagator produces a W angular distribution of approximately the form $dN/d\cos\theta^* \sim (1 - |\cos\theta^*|)^{-1}$, where θ^* is the polar angle [1] of the W in the center-of-mass (c.m.) frame of the W +jet system. This distribution is expected to be similar to that for photon+jet events, which are also dominated by quark propagator diagrams (predominantly $gq \rightarrow \gamma q$). Dijet events, dominated by gluon propagator diagrams (e.g. $gg \rightarrow gg$), are expected to have a distribution of the form $dN/d\cos\theta^* \sim (1 - |\cos\theta^*|)^{-2}$, which is significantly more peaked in the forward/backward direction.

We present a measurement of the W angular distribution in W +jet

events ($dN/d\cos\theta^*$), and compare it with leading order (LO) and next-to-leading order (NLO) perturbative QCD predictions. We also compare $dN/d\cos\theta^*$ measured for W +jet events to previous CDF measurements of dijet [2] and photon+jet [3] events. This measurement represents a significant increase in both the c.m. energy and the number of events compared to a similar measurement presented by the UA1 collaboration [4]. The $W \rightarrow e\nu$ data sample corresponds to an integrated luminosity of $22.8 \pm 0.7 \text{ pb}^{-1}$.

A detailed description of the CDF can be found elsewhere [5]. The components of the detector relevant to this analysis are described briefly here. The Central Tracking Chamber, which is immersed in a 1.4 T solenoidal magnetic field, measures the momenta and trajectories of charged particles in the region $|\eta| < 1.1$ (where $\eta \equiv -\ln \tan(\theta/2)$) [1]. In the central region ($|\eta| < 1.1$), scintillator-based electromagnetic (EM) and hadronic (HAD) calorimeters are arranged in projective towers, each covering $\Delta\eta \times \Delta\phi \approx 0.1 \times 15^\circ$. The central electromagnetic strips are multiwire proportional chambers embedded in the central EM calorimeter at a depth corresponding to shower maximum. Gas-based calorimeters, HAD and EM, cover the region $1.1 < |\eta| < 4.2$ with towers of size $\Delta\eta \times \Delta\phi \approx 0.1 \times 5^\circ$.

The events used in this analysis were accepted using a high- p_T electron trigger (where p_T is the momentum transverse to the beam axis). The trigger requirements and offline cuts used to define an electron candidate are the same as those described in [6]. The electron energy, E , was corrected for detector effects [7] and required to satisfy $E_T > 20 \text{ GeV}$ ($E_T \equiv E \sin\theta$). The electron was also required to satisfy

$|\eta| < 0.95$. Events are weighted to correct for η -dependent electron identification efficiencies [8] (this correction has a negligible effect on $dN/d\cos\theta^*$).

W boson events were selected by requiring the corrected missing E_T ($\vec{E}_T \equiv |\vec{\mathbb{E}}_T|$) to be greater than 20 GeV. Missing E_T , which is an estimate of the transverse momentum of the neutrino, is defined by

$$\vec{E}_T = - \sum_i E_T^i \hat{\mathbf{n}}_i, \quad i = \text{calorimeter tower number with } |\eta| < 3.6,$$

where $\hat{\mathbf{n}}_i$ is a unit vector perpendicular to the beam axis and pointing at the i^{th} calorimeter tower. The missing E_T is corrected for the detector response to the electron, hadronic jets, and low- p_T hadrons; this correction is described in more detail elsewhere [6]. Events consistent with Z boson decay or photon conversion were removed. The transverse mass of the electron–neutrino system (m_T) was required to be greater than 20 GeV/c^2 , where m_T is the invariant mass calculated using only the transverse components of the electron and neutrino momenta.

The events were required to contain at least one jet. A jet is defined as a cluster of energy in the calorimeters (not including the electron); the clustering algorithm is described in detail elsewhere [9]. The jet momentum is defined by $\sum_i E^i \hat{\mathbf{o}}_i$, where the sum is over all calorimeter towers inside a cone of radius $R = 0.7$ ($R \equiv \sqrt{\Delta\eta^2 + \Delta\phi^2}$), and $\hat{\mathbf{o}}_i$ is a unit vector pointing from the event vertex to the i^{th} calorimeter tower. The jet momentum is then corrected for the detector response [10], which is a function of the jet p_T and the jet η . The events are required to contain at least one jet with corrected $p_T > 15 \text{ GeV}/c$. The electron is required to be separated by at least $R = 0.9$

from all jets with corrected $p_T > 15$ GeV/c. This W+jet sample contains 2779 events.

The longitudinal component of the neutrino momentum (p_z^ν) cannot be measured, as particles exiting the detector with large $|\eta|$ can carry high longitudinal momenta. However, if we assume the mass of the electron–neutrino system to be equal to the W boson mass (taken to be 80 GeV/c²), then p_z^ν is restricted to two possible values. When the transverse mass is greater than 80 GeV/c², the two p_z^ν solutions have imaginary components. In such events, the constraint is made to the value of the transverse mass instead of to 80 GeV/c² [11, 8]. A LO Monte Carlo [12] calculation predicts that the fraction of events having one solution that is unphysical is 7×10^{-6} . There are no such events in the data. We then select one of the two solutions, and use that solution to define the c.m. variables. In the Collins–Soper [13] rest frame of the W boson, the two solutions for $\cos \alpha$ (where α is the angle between the electron and the positive z-axis) are equal and opposite. For W[−] bosons we select the solution with positive $\cos \alpha$, and for W⁺ bosons we select the solution with negative $\cos \alpha$. This method was motivated by Monte Carlo studies indicating that the W bosons produced in the Tevatron should be highly polarized, and that the selected event solution is the correct choice in approximately 73% of the events [8]. Since the selected event solution is so often correct, distributions made with it will approximate the true physical distribution. The results presented in this Letter do not rely on this assumption: the same selection method is also used in the theoretical predictions that we compare to the measurement.

Analogous to previous measurements for dijet [2] and photon+jet [3] events, the

hard scattering system is taken to be the W boson and the highest- p_T jet. The c.m. frame of this system is defined using the Collins-Soper [13] prescription: the Lorentz-boost is done in two parts, first along the z -axis, and then in the transverse plane. In order to make the measurement in a region of flat acceptance, the events are required to satisfy three final cuts. We require $|\cos \theta^*| < 0.9$: Monte Carlo studies [8] indicate that to extend this range any further would limit the statistical power of the measurement due to an invariant mass cut ($m^* > 121.5 \text{ GeV}/c^2$) on the W +jet system that removes the $\cos \theta^*$ dependent acceptance caused by the p_T requirement on the jet. The third cut is on the z -component of the boost into the c.m. frame, which is required to have $\gamma_z < 2.35$ and corresponds to a change in rapidity of 1.5.

The final event sample for this analysis is 979 events.

The method used to select one of the two event solutions introduces a smearing in $dN/d\cos \theta^*$. A comparison, using Monte Carlo events, between the selected $\cos \theta^*$ distribution and the true $\cos \theta^*$ distribution generated by the Monte Carlo program is given in Fig. 1(a). There is a migration of events from positive to negative $\cos \theta^*$. In making this figure, $\cos \theta^*$ for W^+ bosons was inverted about zero. Figure 1(b) shows, using Monte Carlo events, a similar comparison between the selected and the true distributions for $|\cos \theta^*|$. In this variable, the distortion due to the solution choice is diminished.

The contamination from electroweak backgrounds was estimated, using the Pythia [14] Monte Carlo program, to be: (i) $W \rightarrow \tau\nu \rightarrow e\nu\nu\nu$: $(3.4 \pm 1.7)\%$; (ii) $Z \rightarrow e^+e^-$: $(1.7 \pm 0.9)\%$; and (iii) $Z \rightarrow \tau^+\tau^-$: $(0.3 \pm 0.2)\%$. The non- W QCD back-

ground was estimated using the transverse mass distribution below 20 GeV/c^2 to be $(4 \pm 4)\%$; the uncertainty is conservatively estimated. The contamination from top quark production, as predicted by the HERWIG [15] Monte Carlo program, would be 7.4% if the top quark had a mass of 130 GeV/c^2 , and falls for higher top quark masses. The effects of the electroweak and QCD backgrounds were subtracted from $dN/d\cos\theta^*$. The result of subtracting the effect of a 130 GeV/c^2 [16] top quark is taken as a systematic uncertainty.

Figure 2 shows $dN/d\cos\theta^*$ for data compared to a LO [12] and a NLO [17] QCD prediction. Each distribution is normalized to have an average value of 1 in the region $-0.6 < \cos\theta^* < +0.6$. The inner error bars indicate the statistical uncertainty (including the normalization uncertainty), and the outer error bars show the statistical and systematic uncertainties combined in quadrature. The systematic uncertainty includes the uncertainties in the background estimates, the calorimeter energy scales, the parton distribution functions, and the QCD renormalization scale. The dominant systematic uncertainty is the uncertainty in the top quark contamination. The data, summarized in Table 1, agree well with the QCD predictions.

In order to compare the theoretical prediction with the data, the following requirements were placed on the Monte Carlo events: (i) electron $p_T > 20 \text{ GeV}/c$, (ii) neutrino $p_T > 20 \text{ GeV}/c$, (iii) electron $|\eta| < 0.95$, (iv) jet $p_T > 15 \text{ GeV}/c$, (v) electron and jets separated by at least $R = 0.9$, (vi) $m_T > 20 \text{ GeV}/c^2$, (vii) $\gamma_z < 2.35$, (viii) $m^* > 121.5 \text{ GeV}/c^2$, and (ix) $|\cos\theta^*| < 0.9$. The two neutrino solutions were found by constraining p_z^ν to the generated mass of the W boson (doing this instead of using

$\cos \theta^*$	$dN/d\cos \theta^*$	Stat err	Sys err
-0.90 to -0.75	4.14	0.38	+0.39 / -0.26
-0.75 to -0.60	1.83	0.23	+0.10 / -0.09
-0.60 to -0.45	1.35	0.19	+0.02 / -0.05
-0.45 to -0.30	1.10	0.17	+0.01 / -0.11
-0.30 to -0.15	0.95	0.16	+0.10 / -0.04
-0.15 to 0.00	0.78	0.14	+0.11 / -0.04
0.00 to 0.15	0.95	0.15	+0.01 / -0.05
0.15 to 0.30	0.96	0.15	+0.06 / -0.04
0.30 to 0.45	0.74	0.13	+0.04 / -0.03
0.45 to 0.60	1.18	0.17	+0.11 / -0.05
0.60 to 0.75	1.48	0.19	+0.15 / -0.04
0.75 to 0.90	2.38	0.26	+0.29 / -0.07

Table 1: The background-subtracted data, normalized to 1 in the region $-0.6 < \cos \theta^* < +0.6$, as displayed in Fig. 2.

a fixed value of 80 GeV/c² has a negligible effect on $dN/d\cos\theta^*$), and the selected solution was defined in the same way as in the data analysis. The measurement resolution on $\cos\theta^*$ ranges from 0.05 at large $|\cos\theta^*|$ to 0.1 near $\cos\theta^* = 0$; its effect on the shape of $dN/d\cos\theta^*$ is negligible (less than 3% in any bin).

Figure 3 shows $dN/d|\cos\theta^*|$ for data compared with the NLO QCD prediction. The data are summarized in Table 2. Also shown in Fig. 3 is $dN/d|\cos\theta^*|$ measured using dijet [2] and photon+jet [3] events. The differences between the photon+jet and W+jet QCD predictions are probably due to the more significant *bremsstrahlung* contribution to photon+jet processes. All three measurements demonstrate good agreement with QCD predictions: the fits have a χ^2/N_{DF} (using the combined statistical and systematic uncertainties) of 13.3/15 for the dijet data; 4.0/7 for the photon data; and 1.3/5 for the W data. The data also indicate a significant difference between the $dN/d|\cos\theta^*|$ distributions for the dijet and W+jet events.

We thank the Fermilab staff and the technical staffs of the participating institutions for their vital contributions. This work was supported by the U.S. Department of Energy and National Science Foundation; the Italian Istituto Nazionale di Fisica Nucleare; the Ministry of Education, Science and Culture of Japan; the Natural Sciences and Engineering Research Council of Canada; the National Science Council of the Republic of China; the A. P. Sloan Foundation; and the Alexander von Humboldt-Stiftung.

$ \cos \theta^* $	$dN/d \cos \theta^* $	Stat err	Sys err
0.00 to 0.15	0.95	0.13	+0.02 / -0.03
0.15 to 0.30	1.05	0.14	+0.03 / -0.02
0.30 to 0.45	1.01	0.14	+0.02 / -0.10
0.45 to 0.60	1.39	0.17	+0.08 / -0.10
0.60 to 0.75	1.82	0.21	+0.14 / -0.11
0.75 to 0.90	3.58	0.35	+0.37 / -0.21

Table 2: The background-subtracted $W+jet$ data, normalized to 1 in the region $|\cos \theta^*| < 0.3$, as displayed in Fig. 3.

References

[^a] Visitor.

- [1] We use a polar coordinate system in which z is along the proton direction, ϕ is the azimuthal angle, and θ is the polar angle.
- [2] CDF Collaboration, F. Abe *et al.*, Phys. Rev. Lett. **62**, 3020 (1989).
- [3] CDF Collaboration, F. Abe *et al.*, Phys. Rev. Lett. **71**, 679 (1993).
- [4] UA1 Collaboration, C. Albajar *et al.*, Z. Phys. C **44**, 15 (1989).
- [5] CDF Collaboration, F. Abe *et al.*, Nucl. Instrum. Methods Phys. Res., Sect. A **271**, 387 (1988).
- [6] CDF Collaboration, F. Abe *et al.*, Phys. Rev. Lett. **66**, 2951 (1991).

- [7] CDF Collaboration, F. Abe *et al.*, Phys. Rev. D **43**, 2070 (1991).
- [8] R.B. Drucker, Ph.D. thesis, University of California at Berkeley, LBL Report No. LBL-34738, 1993 (unpublished).
- [9] CDF Collaboration, F. Abe *et al.*, Phys. Rev. D **45**, 1448 (1992).
- [10] CDF Collaboration, F. Abe *et al.*, Phys. Rev. Lett. **69**, 2896 (1992).
- [11] The transverse mass drops off sharply above $80 \text{ GeV}/c^2$; therefore, recovering these events in this manner does not bias $dN/d\cos\theta^*$ significantly.
- [12] VECBOS, a LO $W + \text{jets}$ Monte Carlo program, described in F.A. Berends, W.T. Giele, H. Kuijf, and B. Tausk, Nucl. Phys. **B357**, 32 (1991).
- [13] J.C. Collins and D.E. Soper, Phys. Rev. D **16**, 2219 (1977);
K. Hagiwara, K. Hikasa, and N. Kai, Phys. Rev. Lett. **52**, 1076 (1984).
- [14] H. Bengtsson and T. Sjöstrand, Comput. Phys. Commun. **46**, 43 (1987).
- [15] G. Marchesini *et al.*, Comput. Phys. Commun. **67**, 465 (1992).
- [16] The current mass limit on the top quark is $131 \text{ GeV}/c^2$. D0 Collaboration, S. Abachi *et al.*, Phys. Rev. Lett. **72**, 2138 (1994).
- [17] DYRAD, a NLO $W + 1 \text{ jet}$ Monte Carlo program including the effects of a second jet, described in W.T. Giele, E.W.N. Glover, and D.A. Kosower, Nucl. Phys. **B403**, 633 (1993).

[18] CTEQ Collaboration, J. Botts *et al.*, Phys. Lett. B **304**, 159 (1993).

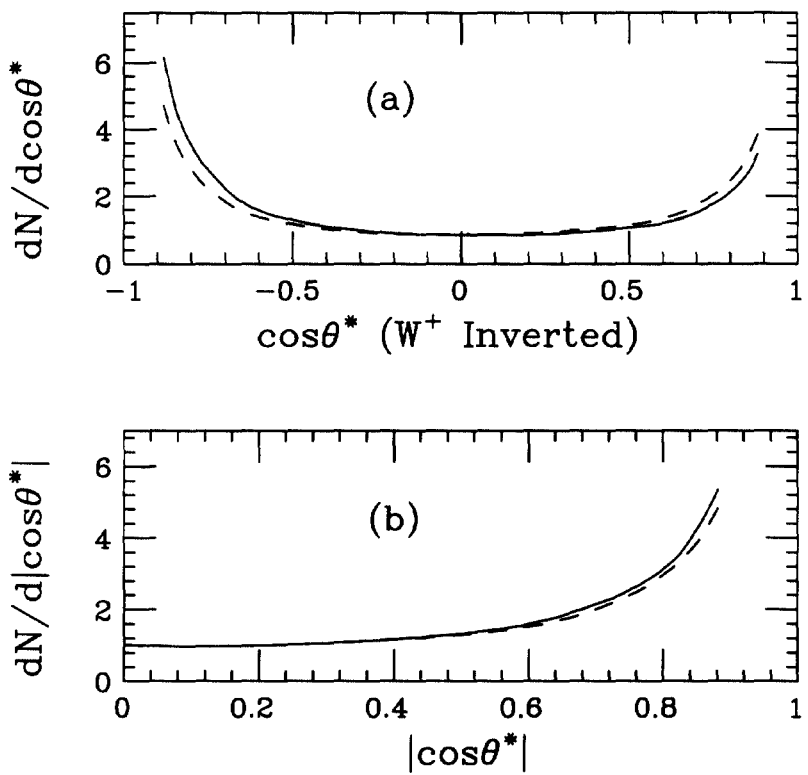


Figure 1: Comparisons between the true $dN/d\cos\theta^*$ as generated by the Monte Carlo program (dashed curves), and $dN/d\cos\theta^*$ obtained by using the selected solution (solid curves) for (a) $\cos\theta^*$ (inverted about zero for W^+ bosons) and (b) for $|\cos\theta^*|$.

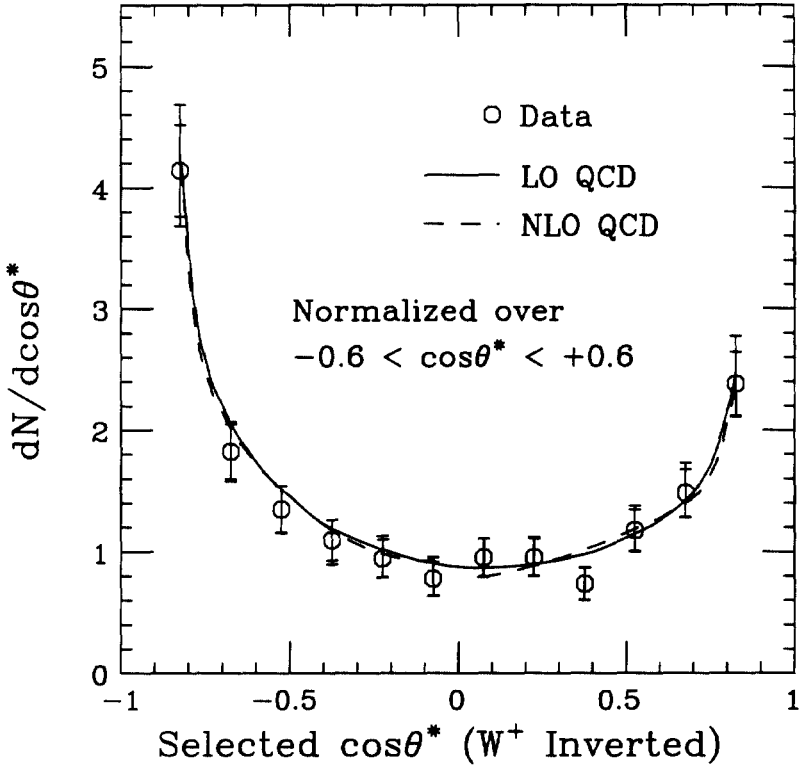


Figure 2: Selected $dN/d \cos \theta^*$ for CDF $W + \text{jet}$ data (circles), compared to a LO (solid curve) and a NLO (dashed curve) QCD prediction. The LO (NLO) theoretical prediction was generated using CTEQ1L (CTEQ1M) [18] parton distribution functions and $p_T/2$ for the renormalization scale. Events containing a W^+ have been inverted about zero. The asymmetry in this variable is predominantly caused by the solution selection procedure. The data and theory predictions are all normalized to have an average value of 1 in the region $-0.6 < \cos \theta^* < +0.6$.

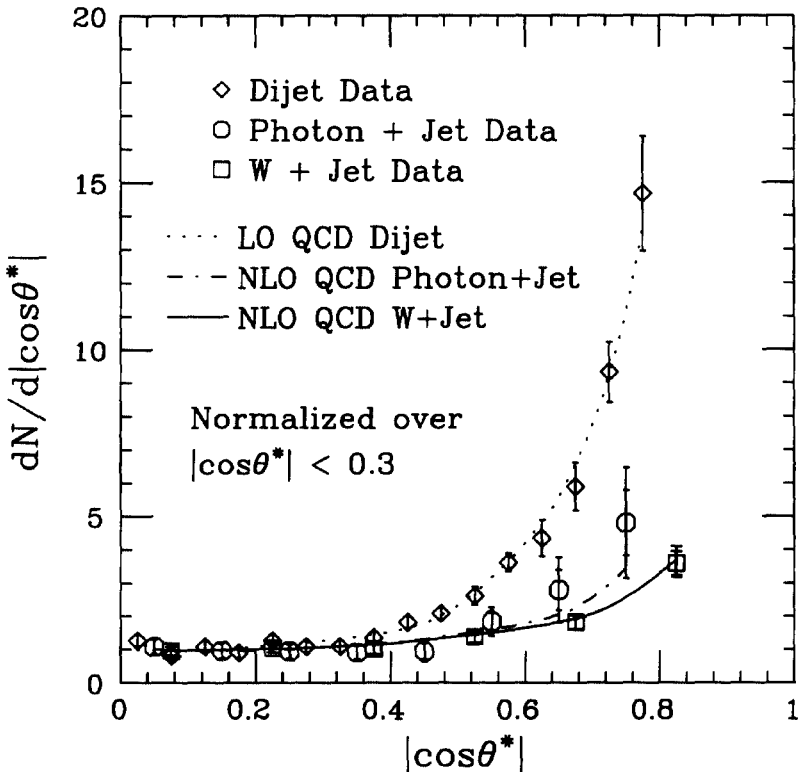


Figure 3: Selected $dN/d|\cos \theta^*|$ for CDF W+jet data (squares), compared to previously published measurements of $|\cos \theta^*|$ for dijet [2] and photon+jet [3] data. NLO QCD predictions are compared with the W+jet (solid curve) and the photon+jet (dashed curve) data. A LO QCD prediction (dotted curve) is compared to the dijet data. The data and theoretical predictions are all normalized to have an average value of 1 in the region $|\cos \theta^*| < 0.3$.